Energy-resolved magnetic domain imaging in TbCo alloys by valence band photoemission magnetic circular dichroism

Pascal Melchior, Markus Rollinger, Philip Thielen, Sabine Alebrand, Ute Bierbrauer, Christian Schneider, Matthias Gottwald, Michel Hehn, Stephane Mangin, Mirko Cinchetti, et al.

Energy-resolved magnetic domain imaging in TbCo alloys by valence band photoemission magnetic circular dichroism

Pascal Melchior,[1,*] Markus Rollinger,[1] Philip Thielen,[1,2] Sabine Alebrand,[1] Ute Bierbrauer,[1] Christian Schneider,[1] Matthias Gottwald,[3] Michel Hehn,[4] Stéphane Mangin,[3,4] Mirko Cinchetti,[1] and Martin Aeschlimann[1]

[1]*Department of Physics and Research Center OPTIMAS, University of Kaiserslautern, Erwin-Schroedinger Strasse 46, 67663 Kaiserslautern, Germany*

[2]*Graduate School of Excellence Materials Science in Mainz, Gottlieb-Daimler-Strasse 47, 67663 Kaiserslautern, Germany*

[3]*Center of Magnetic Recording Research, University of Califonia, San Diego, California 92093-0401, USA*

[4]*Institut Jean Lamour, UMR CNRS 7198, Université de Lorraine, F-54505 Vandoeuvre-lès-Nancy, France*

(Received 23 April 2013; revised manuscript received 13 August 2013; published 18 September 2013)

We report magnetic domain imaging of a terbium cobalt (TbCo) alloy thin film with a high perpendicular magnetic anisotropy in one- and two-photon photoemission electron microscopy (PEEM). Both photoemission processes deliver a clear magnetic circular dichroism (MCD) whose strength is strongly energy dependent. Comparing the energy dependence of the MCD signal in one- and two-photon photoemission, we conclude that the magnetic contrast is mainly an initial state effect. Our results ultimately show that MCD contrast can be obtained in PEEM in valence band photoemission from a material supporting all-optical magnetization switching. This opens the way for the investigation of the all-optical switching process with simultaneous ultrahigh temporal and spatial resolution.

DOI: 10.1103/PhysRevB.88.104415 PACS number(s): 79.60.−i, 78.20.Ls, 75.60.Ch, 75.50.Kj

I. INTRODUCTION

The demand for more efficient data storage devices (faster and smaller) has triggered rapid progress in the field of thin-film magnetism during the last decade. Currently available hard disk drives usually encode information in form of bits in the magnetic state of a ferromagnetic material. Therefore the development of methods for the characterization of the domain formation on a nanometer scale is an urgent subject especially for further improvements of high-density and high-speed recording media. In order to decrease the bit size in magnetic data storage devices for higher data densities, a large perpendicular magnetic anisotropy is needed to maintain signal-to-noise ratio and thermal stability. In this context, the rare-earth transition metal alloys have attracted special interest because they support the effect of all-optical magnetization switching.[1] Here, the direction of magnetization can be reversed directly by single ultrashort laser pulses without any need for an additional external magnetic field.[2] While the underlying physical mechanism is currently under intense investigation, this finding might pave the way for data storage devices in which the magnetic information can be written on the picosecond or even femtosecond time scale.[3,4]

Nowadays, there exist several microscopy techniques to investigate magnetic domain formation on a nanometer scale. One of the most suitable methods is based on the effect of magnetic circular dichroism (MCD). The MCD effect is well established in the x-ray regime (XMCD) at laboratories with access to synchrotron radiation. In combination with a photoemission electron microscope (PEEM), magnetic domains can be imaged with a spatial resolution of a few nanometers.[5,6] As XMCD addresses the core level states of the materials, this technique delivers information about the element specific magnetic properties of magnetic compounds.

In contrast, using light with photon energies in the range of the sample's work function or even below, threshold photoemission MCD addresses the valence band structure near the Fermi energy. This is of special interest because strong optical excitation allows not only to obtain all-optical magnetization switching but also to trigger ultrafast demagnetization. Up to now, this aspect has been approached mostly in time-resolved magneto-optical Kerr effect (MOKE) measurements.[7] Those experiments, however, are not performed with spatial resolution as provided by PEEM. So far, there are only few reports about MCD measurements using ultraviolet or even visible laser pulses.[8–12] Schneider *et al*. investigated the role of exchange interaction and spin-orbit coupling in valence band photoemission from fcc cobalt films at an excitation energy of 23 eV. They found a clear energy dependent MCD signal that varies strongly in the regime of 2 eV below the Fermi energy.[8] This effect has been further investigated at various photon energies between 6 and 24 eV.[9] The observed magnetic dichroism, its energy dependence, and the photon energy dispersion could be explained on the basis of direct transitions in a bulklike band structure of Co. Importantly, Kuch *et al*.[9] were able to demonstrate that the valence band MCD can be explicitly linked to the valence band spin polarization (SP). MCD has been observed also in threshold photoemission and in two-photon photoemission by using visible and ultraviolet laser light, for example, to study the Heusler compounds Ni_2MnGa and Co_2FeSi and also the perpendicularly magnetized 12 ML Ni/Cu(001) system.[10,13,14] The Heusler compounds showed MCD asymmetry values up to 3.5×10^{-3}, whereas for Ni the MCD contrast was around 10% in a very small energy range near the Fermi edge. This MCD contrast was high enough to image the magnetic domains with PEEM.[15,16] Further reports about Co/Pt(111) show similar values for the MCD contrast near the Fermi level.[11,12] In these works, energy resolution has been realized by tuning the work function of the material. However, changing the work function to get the energy information has the drawback that the resulting spectra are always integrations over the whole accessible energy range. True energy-resolved measurements where the kinetic energy of the electrons is detected by an

energy analyzer are of great interest as they directly include the information about the involved electronic states.[17]

Here, we report energy-resolved imaging of magnetic domains in a material with large perpendicular magnetic anisotropy supporting all-optical switching, namely, $Tb_{26}Co_{74}$ alloy thin films.[22] The energy-resolved imaging is obtained using MCD in one- and two-photon photoemission (1PPE and 2PPE). We record the kinetic energy of the photoemitted electrons with a time-of-flight delay-line detector and find that the MCD contrast depends strongly on the electron energy and inverts sign within the photoemission spectrum. The comparison between the energy dependence of the MCD contrast in 1PPE and 2PPE allows us to attribute the origin of the MCD effect to an initial state effect. Uncovering the origin of MCD in TbCo opens the way for the investigation of all-optical switching of the magnetization in rare-earth transition-metal alloys by means of time- and energy-resolved PEEM.

II. EXPERIMENT

For the magnetic domain imaging, we use a photoemission electron microscope (IS-PEEM, Focus GmbH) located in an ultrahigh vacuum (UHV) chamber with a base pressure below 10^{-10} mbar. Its electrostatic lens system offers a spatial resolution of 25–30 nm, hence a way to enable microscopic magnetic imaging far beyond the optical diffraction limit. As detector system, we use a time-of-flight delay-line detector (ToF-DLD).[18,19] The ToF-DLD collects the spatial distribution of the photoelectrons and simultaneously determines their kinetic energy. As we will discuss later, this allows to gain information about the spatial distribution of the MCD asymmetry by just performing two measurements with right (σ^+) and left circularly (σ^-) polarized light.

The spin-resolved measurements are performed in the setup described in Ref. 20 by means of a commercial cylindrical sector analyzer (CSA 300, Focus GmbH) equipped with an additional detector for spin-polarized electrons based on spin-polarized low-energy electron diffraction (SPLEED). The energy resolution was roughly 150 meV. The acceptance angle of the analyzer is $\pm 13^\circ$. The orientation of the sample is 45° with respect to the laser beam, and electrons are detected in the normal-emission geometry.

As light source for the PEEM experiments we use a commercial mode locked Ti:Sapphire laser oscillator with a repetition rate of 80 MHz delivering pulses of a duration of 25 fs. We used the frequency doubled fundamental mode with a photon energy of $h\nu = 3.1$ eV. The high peak power of the laser pulses enables a two-photon photoemission process. The linearly polarized light passes a quarter-wave plate and is focused onto the sample. While keeping the magnetization unchanged, we adjust the angle of the quarter-wave plate to create σ^+ and σ^- light. The magnetic circular anisotropy $A(E,\mathbf{r})$ is then calculated by the following formula:

$$A(E,\mathbf{r}) = \frac{I_{\sigma^+}(E,\mathbf{r}) - I_{\sigma^-}(E,\mathbf{r})}{I_{\sigma^+}(E,\mathbf{r}) + I_{\sigma^-}(E,\mathbf{r})}, \tag{1}$$

with $\mathbf{r} = (x,y)$ in the sample plane. The sample shows an out-of-plane magnetic anisotropy, i.e. along the z direction. Since MCD scales with the projection of the light wave vector $\mathbf{k}$ to the magnetization direction, a light wave vector normal to the sample surface is favorable. This has been realized by the integration of an optical mirror inside the PEEM column to perpendicularly impinge the laser beam onto the sample. The maximum angle between the $\mathbf{k}$ vector of light and the surface normal is approximately four degrees.

The sample was a 20-nm-thick amorphous $Tb_{26}Co_{74}$ film that was grown on a glass substrate with an additional 5-nm-thick tantalum adhesion layer. To prevent oxidation of the film during transport the sample was capped with an aluminum layer of 5 nm. Before starting the measurement, the protection layer was removed in the UHV chamber by argon ion sputtering. The cobalt sample for the spin-resolved photoemission experiments consists of a 10-nm-thin film grown epitaxially on a Cu(001) substrate as reported by Andreyev *et al.*[21]

Figure 1 shows an energy integrated circular anisotropy image $A(\mathbf{r})$ of a multidomain state of the TbCo film excited with a photon energy of 3.1 eV. The observed multidomain state has been induced by temporarily approaching a permanent magnet. The growth and size of the domains have also been checked in magneto-optical microscopy in Faraday geometry[22] and correspond to the domains observed with PEEM. Due to the high symmetry of the experimental configuration (normal incidence of the photons and out-of-plane magnetic anisotropy), we calculate the averaged MCD contrast as the averaged difference between the asymmetries of two areas of interest of equal size, chosen on two domains with opposite magnetization:

$$\mathrm{MCD} = \tfrac{1}{2}(A^{\uparrow} - A^{\downarrow}). \tag{2}$$

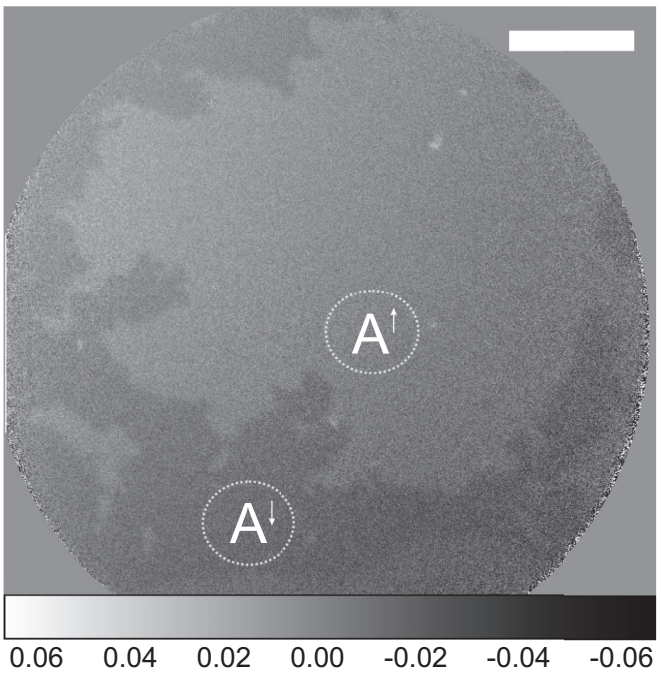

FIG. 1. Circular anisotropy image $A(\mathbf{r})$ of a multidomain state of the TbCo film integrated over the full electron spectrum. The areas labeled with $A^{\uparrow}$ and $A^{\downarrow}$ indicate the integration regions used to calculate the averaged MCD asymmetry in Eq. (2). The white bar indicates a length of 10 μm.

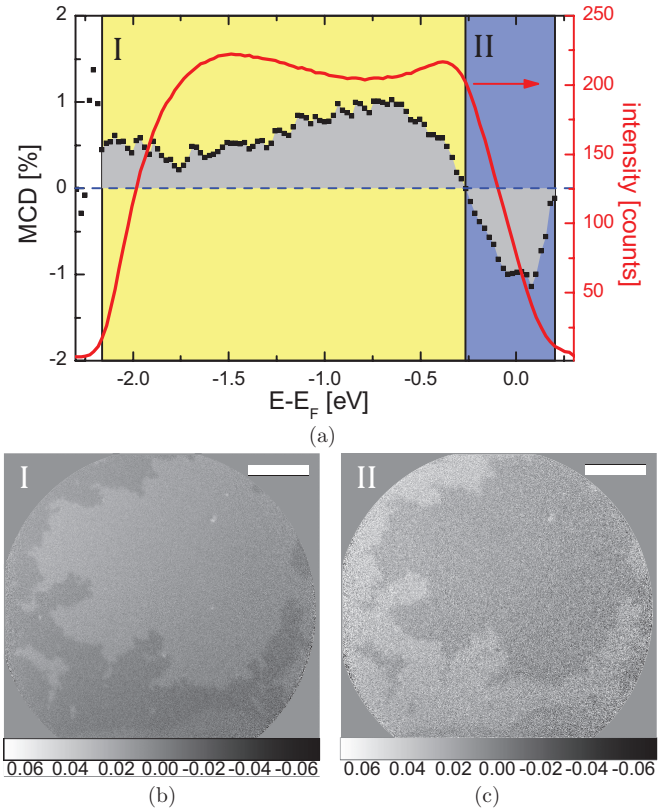

FIG. 2. (Color online) (a) Two-photon photoemission spectrum (red solid line) and corresponding energy dependent MCD contrast (black symbol data) for the excitation with laser pulses of an energy of $h\nu = 3.1$ eV. The energy dependent MCD is calculated via Eq. (2) using the areas shown in Fig. 1 labeled $A^{\uparrow}$ and $A^{\downarrow}$. (b) and (c) Circular anisotropy images $A(\mathbf{r})$ integrated over the energy ranges I and II indicated in (a). The white bar indicates a length of 10 μm.

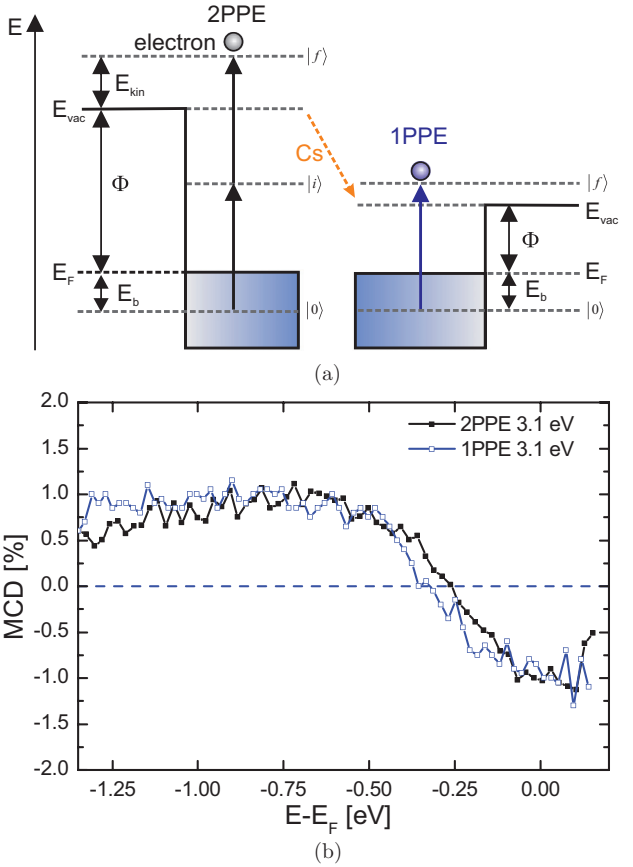

FIG. 3. (Color online) (a) Schematic illustration of the photoemission process before and after reduction of the work function by Cs deposition. (b) MCD asymmetry for 2PPE and 1PPE taken with a photon energy of 3.1 eV (squares).

The integration areas $A^{\uparrow}$ and $A^{\downarrow}$ are indicated by the circles in Fig. 1 while the superscripts $\uparrow$ and $\downarrow$ denote the direction of the magnetization of the corresponding domains. We obtained MCD = 0.65%.

Figure 2(a) shows the photoemission spectrum recorded with $h\nu = 3.1$eV spatially integrated over the image in Fig. 1. With this photon energy, a two-photon photoemission process (2PPE) is needed to create free electrons. This is confirmed by the quadratic power dependence of the photoemission yield on the laser intensity (not shown). The work function Φ of the sample extracted from the 2PPE spectra is approximately 4.1 eV. Furthermore, the photoelectron spectrum shows a peak at an energy of $E - E_F \approx -0.4$ eV below the Fermi level, which has the same energetic position as the Co 3d band with Δ_5 symmetry that dominates the 2PPE spectra of Co/Cu(100) thin films.[21] The symbol data in Fig. 2(a) show the energy dependent MCD contrast extracted from the same regions of interest ($A^{\uparrow}$, $A^{\downarrow}$) as in Fig. 1. The energy dependence follows a characteristic shape of an MCD signal with two peaks of opposite sign.[8,9,23] The negative one coincides with the Fermi edge, while the second peak at a binding energy of 0.65 eV has a positive MCD value and is rather broad. The absolute value of maximum asymmetry is 1.1 % for both peaks. Figure 2(b) and 2(c) show the asymmetry images $A(\mathbf{r})$ integrated over the energy regions I and II, color coded in Fig. 2(a). Region I defines the energy regime from -2.15 to -0.25 eV (region with positive MCD), whereas II is the integration region from -0.25 to 0.2 eV (negative MCD). Note that the weaker signal-to-noise ratio of the image in Fig. 2(c) around the Fermi energy can be attributed to the low photoemission yield at the corresponding energy.

In order to reduce the work function Φ of the material, cesium was deposited on the sample's surface. It should be mentioned that the Cs adsorption is known to have a negligible influence on the bulk electronic structure and the bulk magnetic properties, at least, this is the case in Co and Ni films.[10,24,25] By reducing the work function to $\Phi \approx 1.7$ eV the laser light with $h\nu = 3.1$ eV creates photoelectrons in a direct one-photon photoemission (1PPE) process, as schematically depicted in Fig. 3(a).

Figure 3(b) summarizes the measured MCD asymmetry for the 2PPE and 1PPE process. Only marginal differences appear in the comparison of 1PPE and 2PPE for this particular photon energy. The agreement is not only qualitative in shape but also quantitative in the MCD values. This agreement of 1PPE and 2PPE is a clear hint that the observed MCD stems from the initial state of the photoemission process, marked with $|0\rangle$ in Fig. 3(a). The intermediate state $|i\rangle$ of the 2PPE process seems to play no important role for the MCD contrast. The dominance of the initial state of a 2PPE process for the

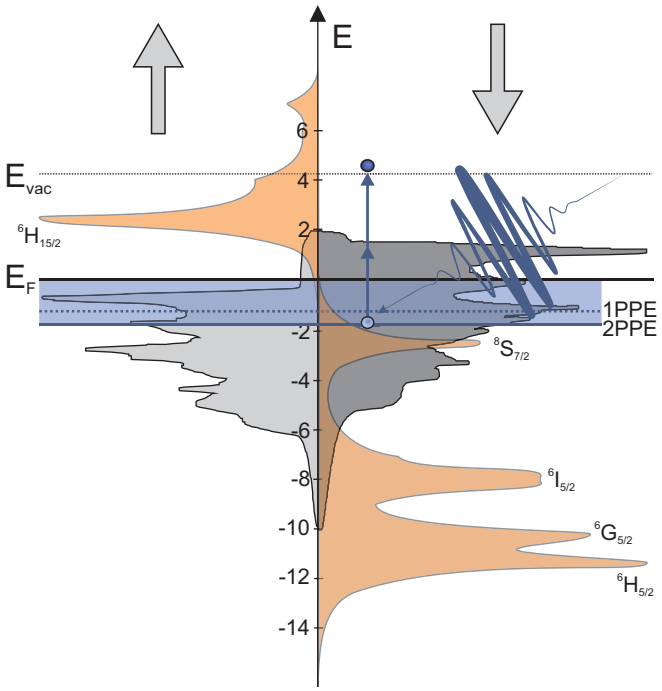

FIG. 4. (Color online) Schematic illustration of spin-resolved density of states of Co 3*d* states[26] (grey) and the 4*f* contribution of Tb[27] (red) in elemental Co and Tb. The blue arrows indicate the 2PPE process with a photon energy of 3.1 eV. The shaded area below the Fermi energy marks the initial states involved in the 1PPE and 2PPE process.

MCD has already been addressed before by Hild *et al.* in a Co/Pt(111) system.[11,12]

III. DISCUSSION

Figure 4 gives a schematic illustration of the density of states of the Co 3*d* states[26] and the Tb 4*f* states in elemental Co and Tb, respectively.[27] The magnetic moment of the rare-earth metals is mainly carried by the localized 4*f* electrons and only a small fraction is delivered by the 5*d* conduction electrons (not shown in Fig. 4).[28] The 4*f* states of the lanthanide materials are closely bound inside the filled 5*s* and 5*p* shells and normally do not contribute to chemical bonding. Therefore, in first approximation, the 4*f* states keep their atomic character also in rare-earth transition-metal compounds. On the other hand, the rare-earth 5*d* electrons are known to hybridize with the 3*d* electrons of the transition metal. This hybridization is ultimately responsible for the antiferromagnetic coupling in TbCo. Elemental terbium shows four well defined 4*f* photoemission multiplets that are formed by spin-orbit coupling.[28,29] The high spin state $^8S_{7/2}$ appears in Tb at a binding energy of $E_b \approx 2.3$ eV (see Fig. 4). It is separated by approximately 4 eV from the other Tb multiplets. This Tb 4*f* state leads to a big absorption cross section for a photon energy of 3.1 eV. However, in the photoemission experiment the work function of the material that reduces the effective probing region has to be considered. The blue shaded area in Fig. 4 marks the initial states accessible by 1PPE and 2PPE spectroscopy in our experiments. In both cases, as shown in Fig. 4, there is only a small overlap between the Tb 4*f*

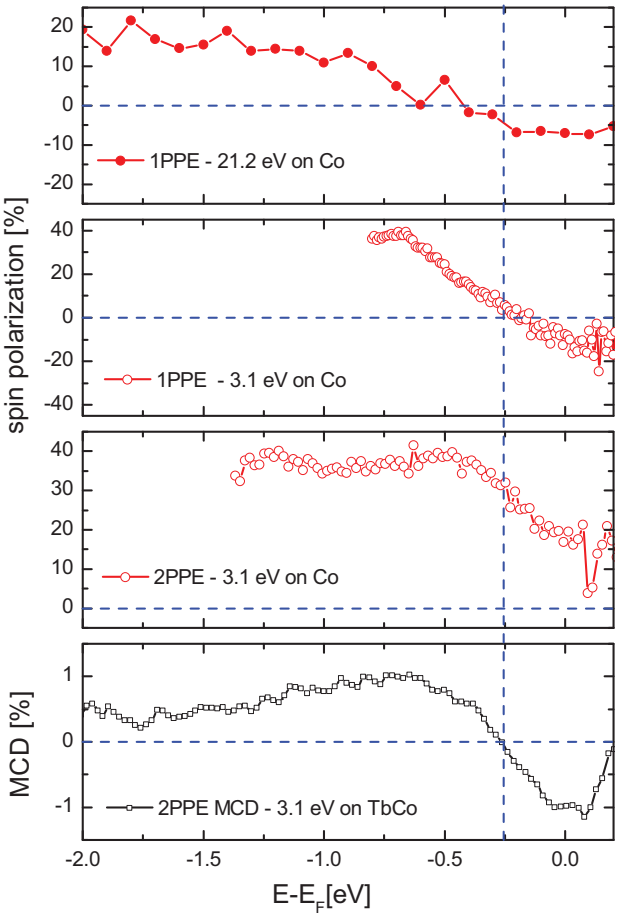

FIG. 5. (Color online) Comparison of MCD signal of TbCo and the spin polarization of fcc Co/Cu(001) for different photon energies.

states and the probing region. Furthermore, XPS spectra on TbFe alloys show that due to the intermixing of Tb and Fe the 4*f* $^8S_{7/2}$ state additionally shifts to larger binding energies.[28] It can be assumed that a similar process also happens in TbCo. Therefore, we conclude that the main contribution to the MCD photoemission signal is delivered by the Co 3*d* states in the valence band of TbCo.

In order to test this hypothesis, we compare our MCD measurements on TbCo with spin-resolved photoemission on pure Co. As already mentioned, Kuch *et al.* have shown that in this case the valence band MCD signal should follow the behavior of the spin polarization (SP).[9] Figure 5 shows the 2PPE MCD of TbCo measured with a photon energy of 3.1 eV below the SP of the Co/Cu(001) film for different excitation energies, namely 21.2 eV from the He I line of a commercial He VUV discharge lamp and 3.1 eV from our laser source. The SP recorded in 1PPE shows the same characteristic sign change as observed in the MCD. The horizontal blue dotted line marks the zero line, the vertical line assigns the energetic position of the MCD sign change. Note that within the energy resolution of the detectors, the change of sign of MCD and SP happens at the same energy. In contrast, the 2PPE measurement shows a purely positive and enhanced SP. This can be explained by the additional spin filter effect due to the spin dependent electron lifetime in the intermediate state of Co populated during the 2PPE process.[24,30] While spin-resolved photoemission

is sensitive to spin-flip scattering in the intermediate state, the MCD photoemission rather probes the spin independent electron population of the intermediate state. Moreover, as already discussed, in the present case, the intermediate state does not significantly influence the MCD signal. On the basis of the experiments of Kuch *et al*., we can thus take the good agreement between the MCD and the behavior of cobalt valence band SP (as detected by 1PPE) as a hint that the MCD signal is mainly dominated by the Co 3*d*-Tb 5*d* hybrid states in the valence band of TbCo. This is of course true only under the assumption that the SP of such hybrid bands is mainly dominated by the Co 3*d* bands or in other words that the hybridization with the Tb 5*d* bands does not significantly change the SP of the Co 3*d* bands.

IV. CONCLUSION

Energy-resolved magnetic circular dichroism measurements in threshold photoemission have been performed on an amorphous $Tb_{26}Co_{74}$ thin film with a strong out-of-plane magnetic anisotropy. The used photoemission electron microscope provides the spatial resolution on the nanometer scale and enables, in combination with a time-of-flight delay-line detector, the energy-resolved imaging of magnetic domains. As light source femtosecond laser pulses with a photon energy of 3.1 eV have been used to generate photoelectrons in 1PPE and 2PPE processes. The circular anisotropy images show a characteristic contrast inversion within the energy spectrum of the photoemitted electrons. We found a perfect agreement of 2PPE and 1PPE MCD spectra for the photon energy of 3.1 eV by reducing the work function through Cs deposition. This indicates that the observed MCD signal is a pure initial state effect for the excitation with this particular photon energy. Furthermore, spin-polarized photoemission spectroscopy measurements reveal a significant agreement of the cobalt valence band SP with the MCD signal. This led us to the conclusion that the observed MCD originates mainly from Co 3*d*-Tb 5*d* hybrid states in the valence band of TbCo, whose spin polarization seems to be dominated by the Co 3*d* bands.

In conclusion, our measurements ultimately show that MCD contrast can be obtained in PEEM in valence band photoemission from TbCo, a material which supports all-optical switching of the magnetization. This opens the way to the investigation of the microscopic mechanism behind the all-optical magnetization switching process with simultaneous ultra-high temporal and spatial resolution.

ACKNOWLEDGMENTS

We acknowledge fruitful discussions with Eric E. Fullerton and the valuable support of Andreas Oelsner (Surface Concept GmbH) for the ToF-DLD. Additionally, we thankfully acknowledge the financial support by the Excellence Initiative (DFG/GSC 266) MAINZ Graduate School for Materials Science in Mainz (to P.T.), the region Lorraine, and the European FP7 Marie Curie grant OP2M.

*melchior@physik.uni-kl.de

[1] C. D. Stanciu, F. Hansteen, A. V. Kimel, A. Kirilyuk, A. Tsukamoto, A. Itoh, and T. Rasing, Phys. Rev. Lett. **99**, 047601 (2007).
[2] L. Le Guyader, S. El Moussaoui, M. Buzzi, R. V. Chopdekar, L. J. Heyderman, A. Tsukamoto, A. Itoh, A. Kirilyuk, T. Rasing, A. V. Kimel *et al*., Appl. Phys. Lett. **101**, 022410 (2012).
[3] K. Vahaplar, A. M. Kalashnikova, A. V. Kimel, D. Hinzke, U. Nowak, R. Chantrell, A. Tsukamoto, A. Itoh, A. Kirilyuk, and T. Rasing, Phys. Rev. Lett. **103**, 117201 (2009).
[4] I. Radu, K. Vahaplar, C. Stamm, T. Kachel, N. Pontius, H. A. Dürr, T. A. Ostler, J. Barker, R. F. L. Evans, R. W. Chantrell *et al*., Nature (London) **472**, 205 (2011).
[5] J. Stöhr, Y. Wu, B. Hermsmeier, M. Samant, G. Harp, S. Koranda, D. Dunham, and B. Tonner, Science **259**, 658 (1993).
[6] G. Schönhense, J. Phys.: Condens. Matter **11**, 9517 (1999).
[7] E. Beaurepaire, J.-C. Merle, A. Daunois, and J.-Y. Bigot, Phys. Rev. Lett. **76**, 4250 (1996).
[8] C. M. Schneider, M. S. Hammond, P. Schuster, A. Cebollada, R. Miranda, and J. Kirschner, Phys. Rev. B **44**, 12066 (1991).
[9] W. Kuch, A. Dittschar, M. Salvietti, M.-T. Lin, M. Zharnikov, C. M. Schneider, J. Camarero, J. J. de Miguel, R. Miranda, and J. Kirschner, Phys. Rev. B **57**, 5340 (1998).
[10] T. Nakagawa and T. Yokoyama, Phys. Rev. Lett. **96**, 237402 (2006).
[11] K. Hild, G. Schönhense, H. J. Elmers, T. Nakagawa, T. Yokoyama, K. Tarafder, and P. M. Oppeneer, Phys. Rev. B **82**, 195430 (2010).
[12] K. Hild, G. Schönhense, H. J. Elmers, T. Nakagawa, T. Yokoyama, K. Tarafder, and P. M. Oppeneer, Phys. Rev. B **85**, 014426 (2012).
[13] K. Hild, J. Maul, G. Schönhense, H. J. Elmers, M. Amft, and P. M. Oppeneer, Phys. Rev. Lett. **102**, 057207 (2009).
[14] T. Nakagawa, I. Yamamoto, Y. Takagi, K. Watanabe, Y. Matsumoto, and T. Yokoyama, Phys. Rev. B **79**, 172404 (2009).
[15] T. Nakagawa, K. Watanabe, Y. Matsumoto, and T. Yokoyama, J. Phys.: Condens. Matter **21**, 314010 (2009).
[16] M. Kronseder, J. Minár, J. Braun, S. Günther, G. Woltersdorf, H. Ebert, and C. H. Back, Phys. Rev. B **83**, 132404 (2011).
[17] T. Nakagawa, I. Yamamoto, Y. Takagi, and T. Yokoyama, J. Electron Spectrosc. Relat. Phenom. **181**, 164 (2010).
[18] A. Oelsner, O. Schmidt, M. Schicketanz, M. Klais, G. Schönhense, V. Mergel, O. Jagutzki, and H. Schmidt-Bocking, Rev. Sci. Instrum. **72**, 3968 (2001).
[19] A. Oelsner, M. Rohmer, C. Schneider, D. Bayer, G. Schönhense, and M. Aeschlimann, J. Electron Spectrosc. Relat. Phenom. **178-179**, 317 (2010).
[20] M. Cinchetti, J.-P. Wüstenberg, M. S. Albaneda, F. Steeb, A. Conca, M. Jourdan, and M. Aeschlimann, J. Phys. D **40**, 1544 (2007).
[21] O. Andreyev, Y. M. Koroteev, M. Sánchez Albaneda, M. Cinchetti, G. Bihlmayer, E. V. Chulkov, J. Lange, F. Steeb, M. Bauer, P. M. Echenique *et al*., Phys. Rev. B **74**, 195416 (2006).
[22] S. Alebrand, M. Gottwald, M. Hehn, D. Steil, M. Cinchetti, D. Lacour, E. E. Fullerton, M. Aeschlimann, and S. Mangin, Appl. Phys. Lett. **101**, 162408 (2012).
[23] J. Henk, J. Phys.: Condens. Matter **13**, 833 (2001).
[24] M. Aeschlimann, M. Bauer, S. Pawlik, W. Weber, R. Burgermeister, D. Oberli, and H. C. Siegmann, Phys. Rev. Lett. **79**, 5158 (1997).

[25]K. Hild, J. Emmel, G. Schönhense, and H. J. Elmers, Phys. Rev. B **80**, 224426 (2009).
[26]V. L. Moruzzi, *Calculated Electronic Properties of Metals* (Pergamon Press, New York, 1978).
[27]S. Lebégue, A. Svane, M. I. Katsnelson, A. I. Lichtenstein, and O. Eriksson, J. Phys.: Condens. Matter **18**, 6329 (2006).
[28]E. Arenholz, E. Navas, K. Starke, L. Baumgarten, and G. Kaindl, Phys. Rev. B **51**, 8211 (1995).
[29]J. K. Lang, Y. Baer, and P. A. Cox, J. Phys. F **11**, 121 (1981).
[30]E. Zarate, P. Apell, and P. M. Echenique, Phys. Rev. B **60**, 2326 (1999).